Extended Abstracts of the 2016 International Conference on Solid State Devices and Materials, Tsukuba, 2016, pp131-132

C-1-05

Autocorrelation Operation using Enhanced Two-photon Absorption Induced Photocurrent in Sub-μm Silicon PIN Waveguide

Guangwei Cong[1], Morifumi Ohno[1], Yuriko Maegami[1], Makoto Okano[1], Koji Yamada[1]

[1]Silicon Photonics Group, Electronics and Photonics Research Institute
National Institute of Advanced Industrial Science and Technology (AIST), Tsukuba, Ibaraki 305-8569, Japan
E-mail: gw-cong@aist.go.jp

Abstract

Optical autocorrelation operation using two-photon absorption (TPA) induced photocurrent in the sub-μm silicon PIN rib waveguide on the 220 nm SOI wafer was for the first time studied by numerical simulation with double input pulses. Strong confinement in this waveguide results in a >60 times photocurrent enhancement compared to the traditional rib waveguide on thick SOI wafers, by which we demonstrated correct pulse width measurement for low power pulses. This work enables us to fabricate the integrated autocorrelator on photonic SOI platforms for weak pulse measurement even without using slow light in silicon photonic crystal waveguides.

1. Introduction

Autocorrelators are widely used in ultrafast optical systems such as ultrafast laser microscopes [1] since optical autocorrelation is one of the most effective methods to measure temporal characteristics of picosecond or femtosecond pulses. Conventional autocorrelators are based on free-space optics components including metal mirrors, nonlinear crystals, and mechanical motors [2]. In comparison, the integrated autocorrelator based on silicon photonic circuits has visible merits including low cost, small size, no mechanical alignment, high stability, etc, so that silicon waveguide based integrated autocorrelators have started attracting research interests [3-5]. So far, two kinds of silicon waveguides and two different mechanisms have been examined for this purpose, the thick rib waveguide using two-photon absorption (TPA) [3] and the photonic crystal waveguides using slow light enhanced TPA [4] and induced third-harmonic generation (SHG) [5]. In addition, photocurrent induced by a single pulse was simulated in Refs. [3,4]. Simulation of autocorrelation operation has not been reported yet, which is useful for studying effective conditions for correct pulse measurement. Since TPA was also observed in sub-μm rib PIN waveguides [6], in this study, we would like to compare the TPA photocurrent sensitivity between the sub-μm rib PIN waveguides on 220 nm SOI (thin rib) and the traditional rib waveguide (thick rib) in Ref. [3] and then performed an autocorrelation simulation using double pulse excitation to demonstrate correct pulse measurement. We expect that the strong confinement in this thin rib waveguide could greatly enhance the TPA sensitivity and thus it can be applied to achieve monolithic integrated autocorrelators on standard photonic SOI platforms for weak pulse measurements which is important for applications in ultrafast laser microscope to analyze biomedical samples.

2. TPA Sensitivity

The studied waveguide structure is shown in Fig. 1(a), which is usually used as PIN phase shifters in silicon photonic circuits and compatible with CMOS process [7]. The corresponding mode profile is also given in Fig. 1(a), which is calculated by FemSIM [8]. The effective mode area (A_{eff}) then can be obtained by the following equation (Eq.) (1).

$$A_{eff} = \frac{(\int E^2\, dA)^2}{\int E^4\, dA} \qquad (1)$$

where E is the electrical field of the mode profile. A_{eff} is calculated to be 0.0875 μm^2. In comparison, the traditional thick rib waveguide has an A_{eff} of 6.2 μm^2 [3]. This small mode area will induce a strong optical confinement which as a result produces larger TPA photocurrents. At the same time, the generated carrier will also result in free carrier absorption (FCA) that intends to reduce the TPA photocurrent. The FCA is not considered in Ref. [3] and assumed fully extracted by reverse bias in Ref. [4]. In this study, we considered FCA effects on TPA sensitivity by introducing the carrier drift time. The simulated device structure is shown in Fig. 1(b) for both the thin and thick rib waveguides.

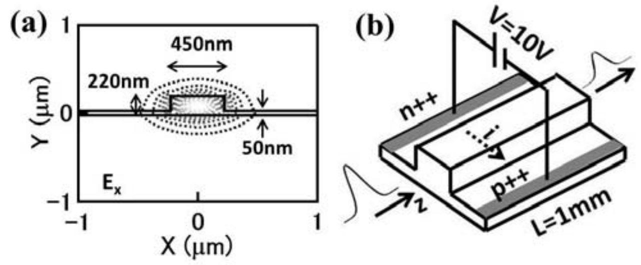

Fig. 1 (a) Cross-section schematic of sub-μm silicon PIN waveguide and its mode profile at λ=1.55 μm for TE polarization. (b) Device structure for pulse propagation simulation with a reverse-bias of 10 V and a device length of 1 mm.

The following Eqs. (2) and (3) describe the effects of TPA, FCA, and linear absorption on the pulse attenuation in waveguide. The symbols can be referred in Refs. [4,9].

$$\frac{dI}{dz} = -\alpha I - \beta I^2 - \sigma N I \qquad (2)$$

$$\frac{dN}{dt} = \frac{\beta A_{eff} I^2}{2\hbar\omega} - \frac{N}{\tau_{dft}} \qquad (3)$$

We solved them in simultaneous iterations by central finite difference method. Then the photocurrent

$$i = \frac{\beta A_{eff} \int I^2 dz}{2\hbar\omega} \qquad (4)$$

can be calculated [4]. Both the intensity I and carrier density N are time and position dependent invariants. To note that in our simulation the waveguide dispersion and free-carrier dispersion were not included because they are negligible for a relatively wide pulse width (2 ps), a short device length (1 mm), and low peak power. As for simulation parameters, absorption coefficient α was set to the propagation loss of -0.1 dB/cm for thick rib and -1.0 dB/cm for thin rib. TPA coefficient β and FCA coefficient σ are 0.6 cm/GW and 1.47×10^{-17} cm^2, respectively [4,9]. τ_{dft} is the carrier drift time that is dominant in biased PIN junctions. For the thin rib waveguide, at a 10 V bias and a pn junction distance d = 2 μm, the electrical field is as large as 5×10^4 V/cm at which the electron drift speed is saturated [10]. So we used an average drift speed of the saturated electron and holes in Ref. [10], 8×10^6 cm/s, which gives τ_{dft} = 25 ps. For the thick rib waveguide, a typical pn junction distance is about 25 μm [11]. In this case, τ_{dft} can be calculated to be ~625 ps using voltage (=10 V) and mobility ($\mu 0$ = 1000 cm^2/V·s). The simulation time was 60 ps and a Gaussian pulse with a 2 ps full width at half maximum (FWHM) was inputted at center.

The peak power (P_{pk}) up to about 60 W has been calculated in order to obviously notice the FCA influence. Fig. 2 shows the photocurrent in the thin rib has greatly enhanced photocurrent compared to the thick one. For the thin rib waveguide, the sensitivity in at lower power side is about 1 mA/W^2, ~66 times higher than that of the thick rib (0.015 mA/W^2). The sensitivity enhancement results from the strong pulse attenuation in the thin rib waveguide. Relative to the ideal power squared line, the photocurrent exhibits a saturation feature with increasing the peak power no matter including FCA or not because at high powers the linear absorption becomes obvious and the pulse is not totally absorbed in the waveguide as short as 1 mm. Furthermore, the FCA induced photocurrent decrease was observed only for the high power excitation. The enhanced TPA sensitivity could enable more effective pulse autocorrelation operation.

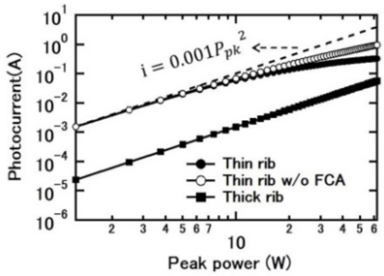

Fig. 2 TPA induced photocurrent at different peak powers.

3. Autocorrelation Operation

It is necessary to verify whether the pulse width can be correctly measured by autocorrelation based on abovementioned thin rib waveguide. The TPA sensitivity discussed above is simulated by inputting a single pulse; while autocorrelation operation can be simulated by inputting double pulses with a delay time. By tuning the delay time, the autocorrelated signal could be obtained. Note that the peak power P_{pk} mentioned below is the sum of peak powers of two pulses to keep consistent with above discussion. Fig. 3(a) compares the autocorrelated signals for a 40 MHz repetition rate with and without FCA at P_{pk} = 12.5 W. In both cases, the autocorrelated widths (FWHMs) are almost same; while FCA induces a relative current decrease on both sides due to the induced FCA by the former pulse for the latter one in the early stage when two pulses are becoming close.

The extracted FWHMs from autocorrelated signals are given in Fig. 3(b), which should be calibrated by the deconvolution factor $\sqrt{2}$ of Gaussian pulse. The corrected measured FWHMs are also shown in Fig. 3(b). As seen, at the low power side, the FWHM is exactly 2 ps and slightly increases with the power. In average, it is about 2.1 ps within a wide power range, which demonstrates a correct autocorrelation operation for 2-ps Gaussian pulses.

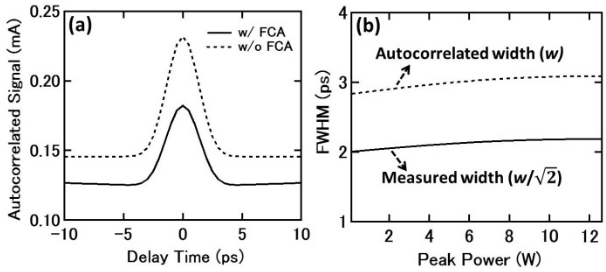

Fig. 3 (a) Autocorrelated signal for 2 ps Gaussian pulses. (b) Pulse width of the autocorrelated signal in (a) and the measured width corrected by the deconvolution factor of Gaussian pulse.

4. Conclusions

TPA induced photocurrent can be >60 times enhanced in the sub-μm silicon PIN waveguide on the 220 nm SOI compared to that on thick SOI wafers. We verified the correct pulse width measurement by autocorrelation operation using this enhanced TPA sensitivity. The integrated autocorrelator based on this PIN waveguide will contribute to the characterization of weak-power ultrafast pulses.

Acknowledgments

This work was supported by JSPS KAKENHI Grant-in-Aid for Young Scientists (B) Grant Number 16K18097.

References

[1] T. Hellerer, Optik & Photonik **4** (2008) 35.
[2] F. Quercioli *et al.*, Opt. Express **12** (2004) 4303.
[3] T. K. Liang *et al.*, Appl. Phys. Lett. **81** (2002) 1323.
[4] R. Hayakawa *et al.*, Appl. Phys. Lett. **102** (2013) 031114.
[5] C. Monat *et al.*, Nature Communications **5** (2014) 3246.
[6] K. Yamada *et al.*, Group IV Photonics, 4th IEEE International Conference on (2007), WP23.
[7] B.G. Lee *et al.*, OFC/NFOEC (2013) PDP5C.3.
[8] ModeSolver FemSIM, https://optics.synopsys.com/rsoft/rsoft-passive-device-femsim.html
[9] A.S. Liu *et al*., Opt. Express **12** (2004) 4261.
[10] S.M. Sze, *Physics of Semiconductor Devices* (2nd), John Wiley & Sons (1981), p46.
[11] D.W. Zheng et al., Opt. Express **16** (2008) 16754.